UNEXPECTED OBSERVATIONS ON THE ACCURACY OF LINEAR COVARIANCE ANALYSIS AND TRACK ASSOCIATION

Alexandra H. Nelson[*], Jackson Kulik [†]

This paper presents two unexpected findings related to the accuracy of linear covariance propagation in astrodynamics. First, higher-dimensional state distributions experience a more rapid deviation from Gaussianity than lower dimensional marginal distributions; in particular, 6-dimensional states diverge from Gaussian behavior significantly faster than 2- or 3-dimensional states. This effect is quantified, and the paper provides information on its underlying causes. Second, it was found that increasing the initial covariance can, in some cases, reduce the non-Gaussianity of the propagated distribution. This counterintuitive behavior is examined in detail, and possible explanations are discussed.

INTRODUCTION

Accurately quantifying and modeling the covariance associated with a spacecraft state is crucial in applications where a spacecraft state needs to be known precisely. This includes space domain awareness (SDA), rendezvous proximity operations (RPO), track association, navigation filters, and many other related applications. In these applications, non-precise covariance models can lead to overconfidence in the spacecrafts predicted state and ultimately mission failure. This paper discusses two anomalies related to linear covariance propagation techniques. These anomalies were studied in the context of track association, but the findings are applicable to various other scenarios.

Linear covariance propagation is a technique commonly used in spacecraft applications to propagate the covariance associated with a state forward in time.[1] Given a mean initial state $\boldsymbol{\mu}_x$ and a previously known covariance $\mathbf{P}_0$ the solution to the dynamical system φ_t can be computed for a given state $\mathbf{x}_t$ as shown in Eq. 1 where φ_t denotes the flow map associated with the dynamical system $\dot{\boldsymbol{x}} = f(\mathbf{x})$.

$$\varphi_t(\mathbf{x}_0) = \mathbf{x}_t \tag{1}$$

We denote the Jacobian ofφ_t evaluated at the mean initial state as the state transition matrix $\mathbf{\Phi}$ as shown in Eq. 2.

$$\mathbf{\Phi}(t, t_0) = \left.\frac{\partial \varphi_t}{\partial \mathbf{x}}\right|_{\boldsymbol{\mu_x}} \tag{2}$$

The state transition matrix and the initial covariance can then be used to propagate the covariance as shown in Eq. 3.

[*]PhD Student, Mechanical and Aerospace Engineering, Utah State University, Logan UT
[†]Assistant Professor, Mechanical and Aerospace Engineering, Utah State University, Logan UT

$$\mathbf{P}_t = \mathbf{\Phi}(t, t_0)\mathbf{P}_0\mathbf{\Phi}(t, t_0)^{\mathbf{T}} \tag{3}$$

Since the state transition matrix gives a linear approximation of the solution flow, the covariance is a linear approximation of the actual covariance. This approximation is appropriate for some space applications, but introduces error. The Gaussian distribution obtained from the linear covariance approximation may not be an accurate approximation of the true distribution.

Several previous studies quantitatively discuss how non-Gaussian the distribution becomes using both Monte Carlo methods and analytical approaches.[2–4] In addition, nonlinear uncertainty propagation methods have been developed to avoid the poor approximations resulting from linear covariance analysis, such as the Gaussian mixture method for uncertainty propagation,[5] polynomial chaos expansion,[6] state transition tensors,[7] unscented transforms,[8] conjugate unscented transformation,[9] and differential algebra.[10]

This paper discusses two unexpected findings that were observed while exploring methods to better perform track association. The first observation was that the non-Gaussianity of the distribution changed with the dimension of the distribution. When the full 6-dimensional state was considered, the non-Gaussianity increased much faster than when a subset of the state variables were considered. As a result, the non-Gaussianity manifests to different degrees in the full distribution as opposed to lower-dimensional marginal distributions.

The second unexpected finding is that downstream non-Gaussianity did not always increase as the initial covariance increased. If the initial uncertainty was higher, one would expect that the non-Gaussianity of the distribution at a later time would also be higher. However, it was observed that inflating the initial covariance in certain ways resulted in a more Gaussian distribution, and linear covariance propagation gave better results under a number of different metrics for identifying non-Gaussianity.

BACKGROUND

Covariance based track association with a Chi-squared test

To determine whether a d-dimensional measurement is statistically consistent with an assumed Gaussian distribution for the spacecraft's state, a one-sided chi-squared test can be performed. This test evaluates the squared Mahalanobis distance D^2 between the measurement and the predicted mean of the state, projected into the measurement space. The result is then compared with the chi-squared threshold $\chi^2_{\alpha,d}$ for a chosen significance level α and degrees of freedom d.

In this formulation, $\mathbf{x}$ is the measurement, $\boldsymbol{\mu_x}$ is the predicted mean state of the spacecraft, and $\mathbf{P_t}$ is the associated covariance. When marginal distributions are considered, the measurement and state are projected into the relevant subspace using a matrix $\mathbf{H}$, which maps the full state to the marginal state of interest. For example, if the measurement concerns only position, $\mathbf{H}$ selects the position components from the full state vector.

The Mahalanobis distance for a full state is then given by Eq. 4 and the Mahalanobis distance for the marginal state is given by Eq. 5.

$$D^2 = (\mathbf{x} - \boldsymbol{\mu_x})^T \mathbf{P_t}^{-1} (\mathbf{x} - \boldsymbol{\mu_x}) \tag{4}$$

$$D_n^2 = (\mathbf{x} - \boldsymbol{\mu_x})^T \mathbf{H}^T (\mathbf{H}\mathbf{P_t}\mathbf{H}^T)^{-1} \mathbf{H} (\mathbf{x} - \boldsymbol{\mu_x}) \tag{5}$$

Comparison of Mahalanobis distance and chi-squared value determines if the measurement is consistent with a distribution.

Hypothesis Test

- If $D^2 > F^{-1}_{\chi^2_{\alpha,d}}$, the observation is inconsistent with the assumed distribution.
- If $D^2 \leq F^{-1}_{\chi^2_{\alpha,d}}$, the observation is not inconsistent with the assumed distribution.

Where F is the Cumulative Distribution Function (CDF).

If the measurement is consistent with the distribution, we do not reject the null hypothesis that the measurement is associated with the given distribution. If the measurement is not consistent with the distribution, we reject the null-hypothesis that this measurement is associated with the given distribution.

Chi-squared tests work if the state has a multivariate normal distribution. This results in the squared Mahalanobis distance having a chi-squared distribution. However, as the distribution becomes less Gaussian, the chi-squared test will pass/fail with an increasingly different ratio than that prescribed by the chosen significance value.

In Gutierrez et al.,[4] the chi-squared test is utilized as a statistical measure to assess the Gaussianity of propagated uncertainty distributions. Specifically, the authors use a Monte Carlo-based Cramér-von Mises (CVM) test to evaluate how closely the distribution of Mahalanobis distances from simulated samples conforms to a theoretical chi-squared distribution. This test provides a scalar metric, ω^2, which quantifies the deviation from a true multivariate Gaussian distribution. A threshold, derived from chi-squared confidence intervals, is then applied to determine when the propagated state uncertainty can no longer be considered Gaussian. This threshold-based evaluation allows the authors to pinpoint the transition to non-Gaussian behavior during orbit propagation. This work does not utilize the same metric. However, the use of Monte-Carlo Chi-Squared based methods to assess the non-Gausianity of the system was inspired by the work of Gutierrez et al.[4]

A Measure of Non-Gaussianity: WUSSOS

Because chi-squared tests can only indirectly assess deviations from Gaussianity, analytical measures such as WUSSOS are valuable for quantifying the sources of nonlinearity. The whitened uncertainty-scaled second-order stretching (WUSSOS) metric is an analytical method used to quantify error that results from linear covariance propagation.[2] WUSSOS uses a whitening transformation on the higher-order terms of the flow map. The Taylor series expansion for the flow map about the mean can be seen in Eq. 6.

$$\boldsymbol{\varphi}(\boldsymbol{\mu_x} + \delta\mathbf{x}) = \boldsymbol{\varphi}(\boldsymbol{\mu_x}) + \boldsymbol{\Phi}\,\delta\mathbf{x} + \frac{1}{2}\left.\frac{\partial^2 \boldsymbol{\varphi}}{\partial \mathbf{x}^2}\right|_{\boldsymbol{\mu_x}} \delta\mathbf{x}^2 + \mathcal{O}(\delta\mathbf{x}^3) \tag{6}$$

The second-order terms of this expansion are denoted as $\boldsymbol{\Psi}$ as shown in Eq. 7.

$$\boldsymbol{\Psi} = \left.\frac{\partial^2 \boldsymbol{\varphi}}{\partial \mathbf{x}^2}\right|_{\boldsymbol{\mu_x}} \tag{7}$$

Then WUSSOS requires an optimization to determine the maximal error in propagating the vectors on the 1-sigma initial covariance ellipsoid relative to the covariance as propagated by linear covariance analysis. The equation for WUSSOS is shown in Eq. 8

$$\max_{\mathbf{x}^T\mathbf{P}_0^{-1}\mathbf{x}=1} \left\|\mathbf{\Psi x}^2\right\|_{\mathbf{P}_t^{-1}} \tag{8}$$

where $\mathbf{\Psi x}^2$ is shorthand notation for the double contraction of the tensor using Einstein notation as defined in Eq. 9

$$\left(\mathbf{\Psi x}^2\right)^i = \left(\mathbf{\Psi}\right)^i_{j,k}\ \mathbf{x}^j\mathbf{x}^k \tag{9}$$

The WUSSOS value can be used to determine the relative non-Gaussianity of the distribution over time because it is an uncertainty scaled measure of the difference between the first and second-order Taylor series approximations. WUSSOS values are typically computed from the full state distribution. However, a marginal WUSSOS value can be obtained using Eq. 10, where H is a matrix that projects the full state onto a marginal subspace. When the marginal distribution corresponds to the position components, we refer to the resulting metric as position WUSSOS.

$$\max_{\mathbf{x}^T\mathbf{P}_0^{-1}\mathbf{x}=1} \left\|\mathbf{H\Psi x}^2\right\|_{(\mathbf{HP}_t\mathbf{H}^T)^{-1}} \tag{10}$$

CASE STUDIES

The following case studies examine the unintuitive findings in detail, quantifying how dimensionality and initial covariance influence the accuracy of linear covariance propagation.

Dimensionality

To explore the non-Gaussianity of a full state distribution as compared with a lower-dimensional marginal distribution, we followed the procedure used by Gutierrez et. al.[4] to quantify non-Gaussianity of a propagated distribution. Ten-thousand random samples were generated for the initial state and covariance shown in Eq. 11. These initial conditions for the mean represent a spacecraft in an equatorial circular orbit with a radius of 6678.0 km where μ is the gravitational parameter $398600.0\text{km}^2/\text{s}^2$.

$$\begin{aligned}\mathbf{x}(0) &= [6678.0\text{km},\ 0\text{km},\ 0\text{km},\ 0\text{km/s},\ \sqrt{\frac{\mu}{6678.0}}\text{km/s},\ 0\text{km/s}] \\ \mathbf{P}(0) &= \text{diag}([0.01\text{km},\ 0.01\text{km},\ 0.01\text{km},\ 10^{-6}\text{km/s},\ 10^{-6}\text{km/s},\ 10^{-6}\text{km/s}])\end{aligned} \tag{11}$$

The mean state and the samples were propagated forward in time using two-body dynamics with no perturbations. The covariance was propagated using linear covariance propagation as shown in Eq. 3 . Then, a chi-squared test associated with the distribution propagated with linear covariance analysis was performed at each time for each propagated sample.

The chi-squared test was performed with the full state vectors as well as with projections of the state into lower dimensions. A threshold of 98.8%, the 3-sigma bound associated with 2-dimensional Gaussian random variable, was applied to each chi-squared test as the significance value. Since the samples came from the initial state distribution, if the linear covariance propagation is entirely accurate in describing the distribution at later time steps and a threshold of 98.8%

is used, it is expected that approximately 98.8% of the samples will pass the chi-squared test. The deviation in the number of propagated samples passing the chi-squared test from this anticipated value gives a measure of the effectiveness of the linear covariance propagation and the resulting non-Gaussianity of the true nonlinearly propagated distribution.

The results of these chi-squared tests over time are shown in Fig. 1. The marginal distributions shown correspond to increasingly higher-dimensional projections: (x) in 1D, (x, y) in 2D, (x, y, z) in 3D, $(x, y, z, \dot{x})$ in 4D, and so on, with each additional dimension incorporating another state variable. All dimensions begin with 98.8% of the samples passing the chi-squared test and being associated with the linear covariance distribution. As the orbit progresses, the percentage of samples associated with the linear covariance distribution decreases. This is expected, as linear covariance propagation becomes a poor approximation for nonlinear systems over time.

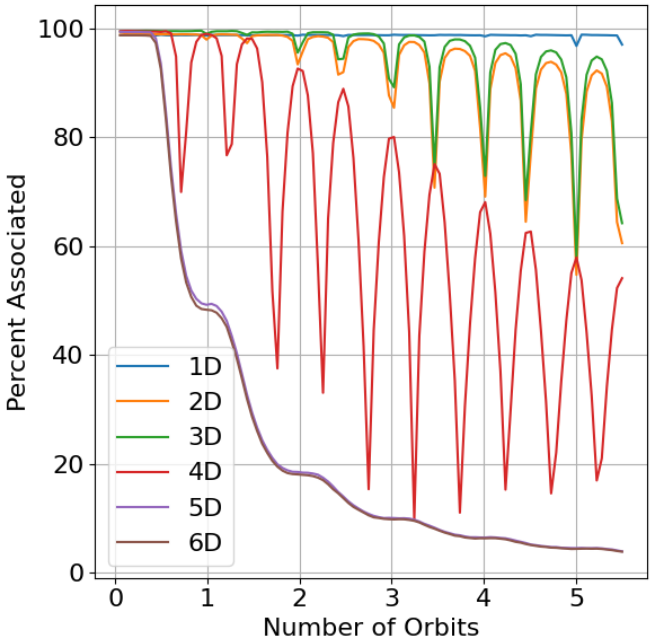

Figure 1: Chi-Squared results for different state dimensions.

An interesting aspect of Fig. 1 is the varying rate at which the percentage of samples associated with the mean decreases. Fig. 1 shows that linear covariance propagation provides a better approximation for lower-dimensional states (2 or 3 dimensions), but the accuracy decreases as the state dimensionality increases.

Next, various permutations of 2D states were studied (e.g., x and y, x and z, x and $\dot{x}$ ...). The 2-dimensional case was chosen due to the in-plane motion of the orbit; if out-of-plane motion is present, a 3-dimensional state representation might be more appropriate. The results of this study are shown in Fig. 2. Note that only the permutations including x are shown in the graph. Other permutations were examined, but the results were very similar, so only the x-based permutations are shown for clarity. This study confirmed that the results in Fig. 1 were not due to a random permutation of states. All 2-dimensional permutations exhibit a slower decrease in accuracy compared to the 6-dimensional state.

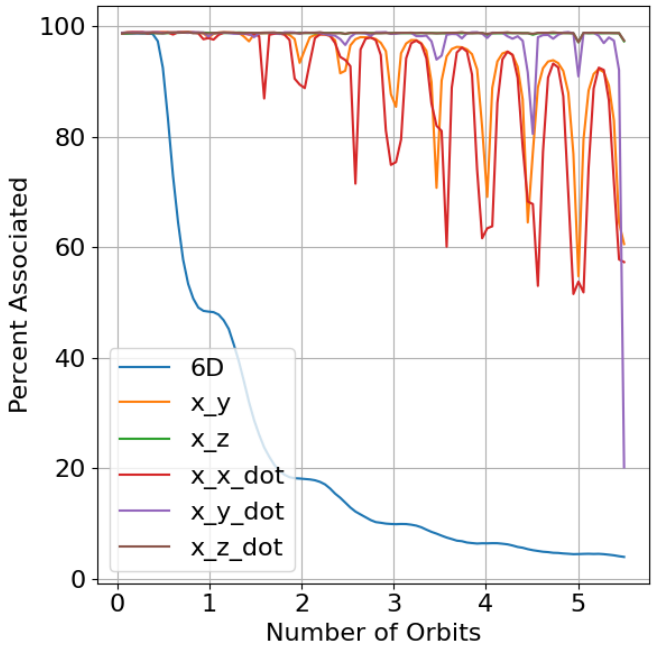

Figure 2: Chi-Squared results for different 2-dimensional states.Illustration Caption Goes Here

While the chi-squared results reveal how often propagated samples remain statistically consistent with a Gaussian assumption, the WUSSOS metric provides an analytical measure of the underlying nonlinearity driving this behavior. To better quantify the nonlinearities in the system, the 2-dimensional and 6-dimensional WUSSOS values were computed, and can be seen in Fig. 6 for a variety of differing initial covariances including the one under study in this section. The 6-dimensional WUSSOS values are several orders of magnitude larger than the 2-dimensional values, indicating significantly greater nonlinearity in the full state space. Since WUSSOS quantifies the degree of nonlinearity in the system, this result suggests that the 6-dimensional system exhibits more pronounced uncertainty-scaled nonlinear behavior than its 2-dimensional projection. This observation is consistent with earlier findings: linear covariance propagation tends to perform better when examining lower-dimensional marginalizations of the full state distribution.

While we are interested in the effects of perturbations to the distribution from unmodeled higher-order terms in the Taylor series, it is illustrative to consider the effect an independent random perturbation instead. Consider two independent distributions such that $x \sim N(0, I_n)$, $y \sim N(0, I_n)$, and $E(xy) = 0$. If the random variable x is perturbed by ϵy for some small parameter ϵ then the new variable is distributed according to $z = x + \epsilon y \sim N(0, (1+\epsilon^2)I_n)$. Next, it can be determined how often z is in the 99% ellipsoid of x using Eq. 12.

$$P\left(\|Z\|^2 \leq F^{-1}_{\chi^2_{0.99,d}}\right) = F_{\chi^2_{0.99,d}}\left(\frac{F^{-1}_{\chi^2_{0.99,d}}}{1+\varepsilon^2}\right) \tag{12}$$

Fig. 3 shows the results of using Eq. 12 for different dimensions (i.e. 1,2, ..., 6). In this figure, one can see that the higher dimensions fall off faster than lower dimensions. This means that a

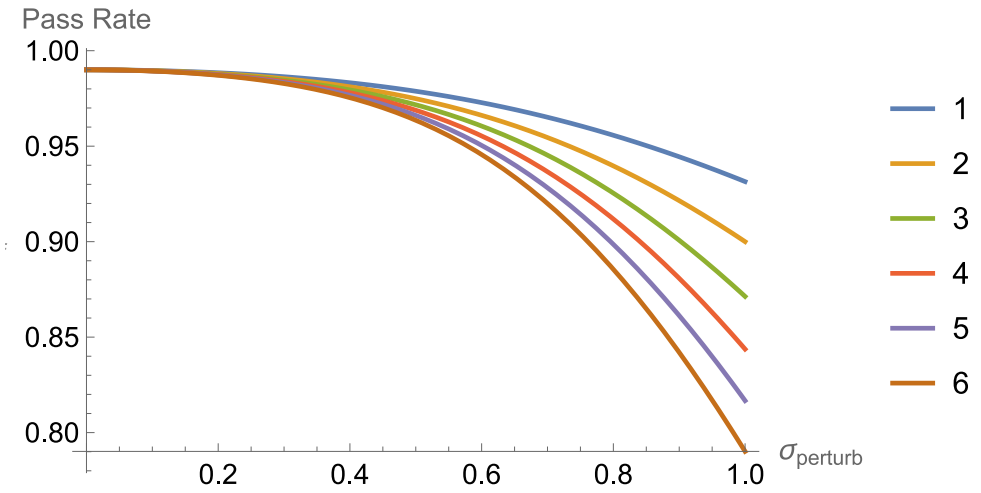

Figure 3: The overlap of x and z ellipsoids in different dimensions

perturbation with the same standard deviation of its marginal distributions, leads to more samples outside of the 99% unperturbed covariance ellipsoid.

The effect described above depends only on the dimension and applies to all distributions. There is an additional affect that is present in heteroscedastic distributions and their marginals. Fig. 4 provides an illustration of this effect. The two ellipses show how a 2D perturbation (red vector) shifts points relative to the ellipsoid. This perturbation can be decomposed into its x- and y-components and these components can be applied independently. The results of applying the x-component individually are shown by the bell curves on the x-axis. In the two-dimensional case, none of the perturbed z-values remain inside the original ellipsoid, whereas in the one-dimensional cases, some overlap persists.

These results highlight the need for caution when applying linear covariance propagation to high-dimensional systems. When computationally feasible, this motivates the need to employ nonlinear uncertainty propagation methods and associated non-Gaussian statistical tests for consistency. Moreover, while marginal distributions may appear approximately Gaussian, the full joint distribution can still exhibit significant non-Gaussianity. This may cause misleading inferences if only marginal views are considered. Therefore, it is important to carefully consider the implications of assessing Gaussianity in the full state distribution versus marginal distributions to determine which is appropriate in context. Lastly, in high-dimensional tracking problems, using chi-squared-based association tests on marginal distributions rather than the full state may improve the ability to avoid rejecting valid track associations (reducing false negative associations beyond the chosen significance value), particularly when the full-state distribution deviates substantially from Gaussian assumptions.

Initial Covariance Effect on Non-Gaussianity

Surprisingly, increasing the initial covariance sometimes results in a higher percentage of samples passing the chi-squared test, indicating that linear covariance propagation is, at times more accurate in a sense, with higher initial uncertainties. The same methodology used in the dimensionality study was applied to a fixed 6-dimensional mean state. This time, the marginal variance for all position components was varied from 0.01 km^2 to 100.0 km^2 as a part of a diagonal covariance matrix and

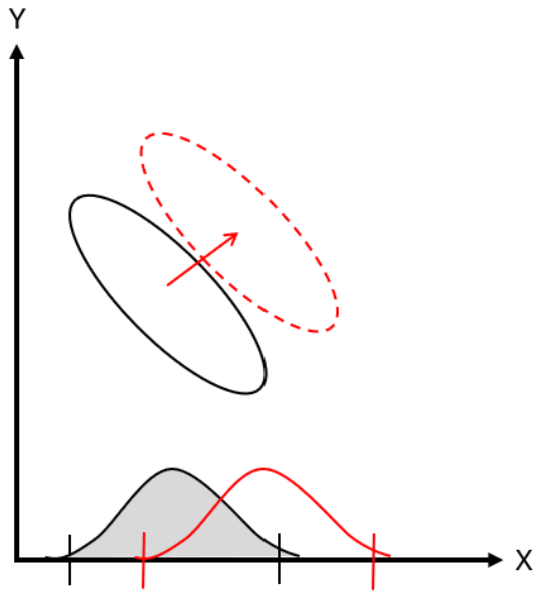

Figure 4: 2-Dimensional vs. 1-Dimensional perturbations

the marginal standard deviations for the velocity components were held constant at 10^{-6}km/s. The same graph was then produced using 2-dimensional marginal positions in the x-y plane. Both graphs can be seen in Fig. 5

In the 6-dimensional plot, a smaller initial position variance of 0.01 km^2 led to inferior chi-squared test performance compared to a 1.0 km^2 variance. This was an unexpected result given the conventional assumption that smaller uncertainties produce more reliable results under linear approximation. To further investigate, a similar analysis was performed using 2-dimensional state projections. This helped isolate whether the effect was related to state dimensionality or a more general property of the dynamics. The 2-dimensional plot showed that overall linear covariance results performed as expected but at half and full orbits the higher initial position variance of 1.0 km^2 and 0.1 km^2 performed better than the 0.01 km^2 initial position variance.

To further explore this effect, WUSSOS values, an uncertainty scaled measure of second-order nonlinearity, were computed for each case. The results of this study are shown in Fig. 6. The WUSSOS plots revealed anomalous behavior at approximately half and full orbital periods, where increased initial covariance did not correspond to higher maximum nonlinearity, contrary to expectations.

First, lets explore why the 0.01, 0.1 and 1.0 variances appear in a none- intuitive order on the 6-Dimensional percent associated plot. This results from the fact that very small variance can occur in directions where the true system dynamics are highly nonlinear. These small variances cause nonlinearities to have a disproportionately large relative effect.

These effects can then be exaggerated when singularities appear in the STM. Previous work discusses these singularities in a variety of different contexts.[11–13] The singularity is the result of the covariance, associated with the velocity, dominating and causing the covariance matrix to be nearly singular as shown in Eq. 13.

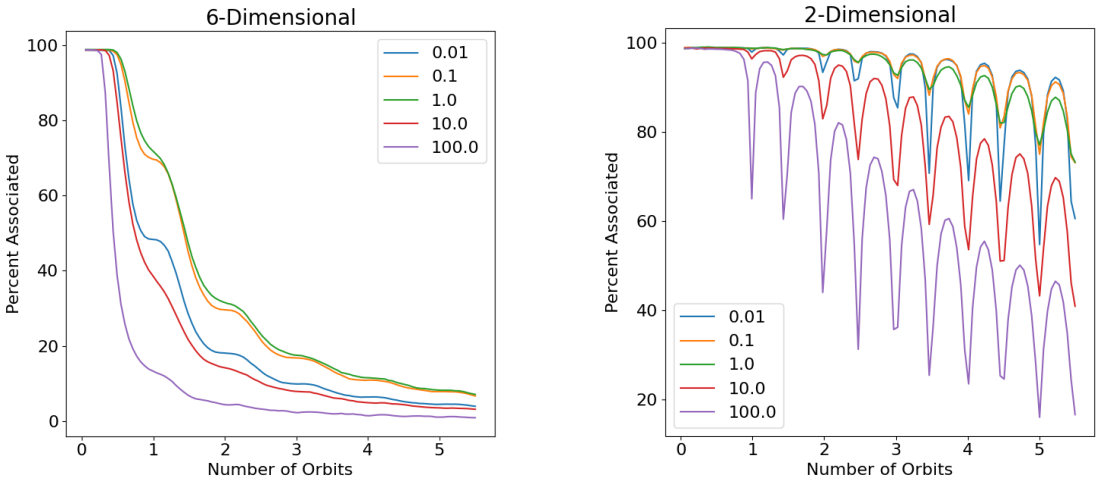

Figure 5: Chi-Squared results for different initial position covariances.

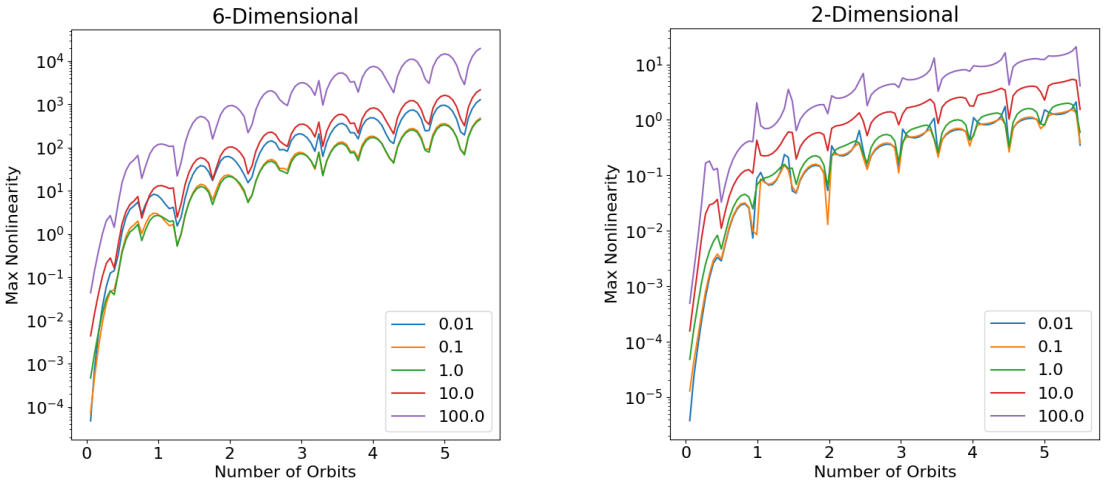

Figure 6: WUSSOS plots for varying initial position covariance.

$$\mathbf{P}_0 = \begin{bmatrix} \mathbf{P^{rr}} & \mathbf{0} \\ \mathbf{0} & \mathbf{P^{vv}} \end{bmatrix} \approx \begin{bmatrix} \mathbf{0} & \mathbf{0} \\ \mathbf{0} & \mathbf{P^{vv}} \end{bmatrix} \tag{13}$$

Using the covariance from Eq. 13 and the STM shown in Eq. 14 the covariance can be found using linear covariance propagation as shown in Eq. 15.

$$\mathbf{\Phi}(t, t_0) = \begin{bmatrix} \mathbf{\Phi^r_r} & \mathbf{\Phi^r_v} \\ \mathbf{\Phi^v_r} & \mathbf{\Phi^v_v} \end{bmatrix} \tag{14}$$

$$\mathbf{P^{rr}_t} \approx \boldsymbol{\Phi}^{\boldsymbol{r}}_{\boldsymbol{v}}(t, t_0)\mathbf{P^{vv}_0}\boldsymbol{\Phi}^{\boldsymbol{r}}_{\boldsymbol{v}}(t, t_0)^T \tag{15}$$

The singularities then occur when the determinant of the upper right block of the STM, $\mathbf{\Phi^r_v}$, is zero. This occurs for times of flight at multiples of 2π and 1.4067, 2.4453, 3.4612, etc. These points are where we see higher initial uncertainties performing better than lower initial uncertainties when examining the position marginal distribution. These singularities accentuate the small initial covariances effect on the distribution. They exaggerate the directional collapse of linear covariance propagation and the breakdown is fundamentally due to the mismatch between assumed linearity and actual nonlinear behavior in low-variance directions.

This result suggests that in some orbital regimes, small initial uncertainties in marginal position may lead to deceptive confidence in the accuracy of linear propagation. The effect of singularities in blocks of the state transition matrix need to be considered when using linear covariance propagation with heteroscedastic initial uncertainty.

CONCLUSION

Accurate covariance propagation is critical for applications such as space domain awareness (SDA), rendezvous proximity operations (RPO), track association, and navigation filtering. While linear covariance propagation is sufficient in some cases, its limitations must be carefully considered in precision-critical applications.

This work examined two key anomalies that influence covariance propagation accuracy. First, dimensionality effects were quantified using WUSSOS and chi-squared tests, showing that high-dimensional state distributions deviate from Gaussianity much faster than lower-dimensional marginals. Specifically, 6-dimensional states exhibited significantly faster degradation of Gaussianity than 2- or 3-dimensional projections. Second, initial covariance effects were analyzed, revealing that larger initial covariances may, in some cases, lead to more Gaussian behavior downstream. This is a result of the small variance and high non-nonlinearities appearing in the same direction. When these directions align, the small variances cause nonlinearities to have a disproportionately large relative effect. These affects can then be exaggerated by singularities in the state transition matrix. These findings highlight the need for caution when applying linear covariance methods, especially in high-dimensional or highly heteroscedastic scenarios.

REFERENCES

[1] D. K. Geller, "Linear Covariance Techniques for Orbital Rendezvous Analysis and Autonomous Onboard Mission Planning," Vol. 29, No. 6, pp. 1404–1414, 10.2514/1.19447.

[2] J. Kulik, B. Hastings, and K. A. LeGrand, "Linear Covariance Fidelity Checks and Measures of Non-Gaussianity," 2025.

[3] M. Mercurio, M. Majji, and P. Singla, "How Non-Gaussian Is It?: Applications to Astrodynamics,"

[4] J. Gutierrez, K. Hill, E. L. Jenson, D. J. Scheeres, J. C. Bruer, and R. D. Coder, "Classifying State Uncertainty for Earth-Moon Trajectories," Vol. 71, No. 3, p. 29, 10.1007/s40295-024-00451-w.

[5] K. J. DeMars, R. H. Bishop, and M. K. Jah, "Entropy-Based Approach for Uncertainty Propagation of Nonlinear Dynamical Systems," Vol. 36, No. 4, pp. 1047–1057, 10.2514/1.58987.

[6] B. A. Jones, A. Doostan, and G. H. Born, "Nonlinear propagation of orbit uncertainty using non-intrusive polynomial chaos," *Journal of Guidance, Control, and Dynamics*, Vol. 36, No. 2, 2013, pp. 430–444.

[7] I. Park and D. J. Scheeres, "Hybrid method for uncertainty propagation of orbital motion," *Journal of Guidance, Control, and Dynamics*, Vol. 41, No. 1, 2018, pp. 240–254.

[8] S. J. Julier and J. K. Uhlmann, "Unscented filtering and nonlinear estimation," *Proceedings of the IEEE*, Vol. 92, No. 3, 2004, pp. 401–422.

[9] N. Adurthi, P. Singla, and T. Singh, "Conjugate Unscented Transformation: Applications to Estimation and Control," Vol. 140, No. 3, p. 030907, 10.1115/1.4037783.

[10] R. Armellin, P. Di Lizia, F. Bernelli-Zazzera, M. Berz, *et al.*, "Nonlinear mapping of uncertainties: a differential algebraic approach," *4th International Conference on Astrodynamics Tools and Techniques (ICATT)*, 2010, pp. 04–29.

[11] J. Kulik and D. Savransky, "Relative Transfer Singularities and Multi-Revolution Lambert Uniqueness," *AIAA SCITECH 2022 Forum*, American Institute of Aeronautics and Astronautics, 10.2514/6.2022-0958.

[12] F.-T. Sun, "On the minimum time trajectory and multiple solutions of Lambert's problem," *American Institute of Aeronautics and Astronautics Conference*, 1979.

[13] H. Chen, C. Han, Y. Rao, J. Yin, and X. Sun, "Algorithm of Relative Lambert Transfer Based on Relative Orbital Elements," Vol. 42, No. 6, pp. 1413–1422, 10.2514/1.G003348.